Supporting Information

Improving Li dendrite suppression capability of garnet solid-state electrolytes by in situ LiF grain boundary modification

Huan Zhao,‡[abcd] Zhihao Guo,‡[acd] Xiaobao Zhang,[acd] Ning Wang,[acd] Yiyang Xiao,[abcd] Shiang Liang,[acd] Weidong Zhuang,[b] Juanyu Yang*[acd] and Xiaowei Huang*[acd]

[a.] *National Engineering Research Center for Rare Earth, Grirem Advanced Materials Co., Ltd., Beijing 100088, China.*

[b.] *School of Metallurgical and Ecological Engineering, University of Science and Technology Beijing (USTB), Beijing, 100083, China.*

[c.] *Rare Earth Functional Materials (Xiong'an) Innovation Center Co., Ltd., Xiong'an 071700, China.*

[d.] *General Research Institute for Nonferrous Metals, Beijing 100088, China.*

E-mail: hxw0129@126.com; juanyuyang@grinm.com

‡ **The authors contributed equally to this work.**

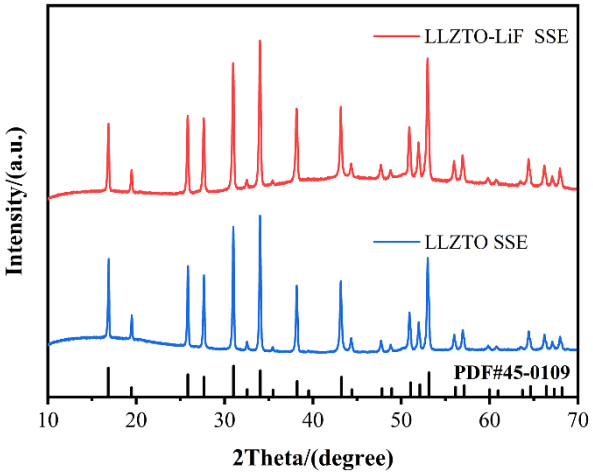

Fig. S1 XRD patterns of LLZTO and LLZTO-LiF SSEs.

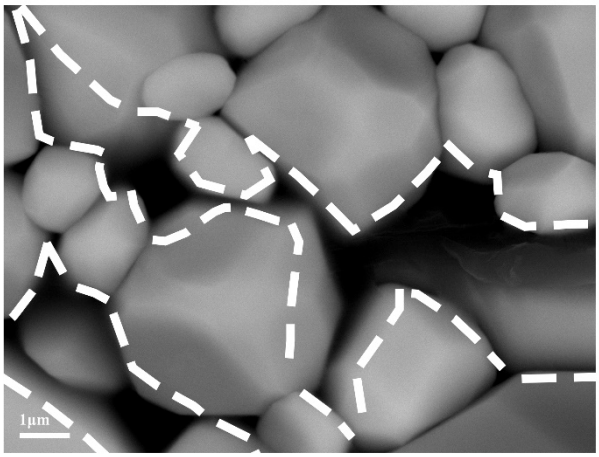

Fig. S2 BSE image of LLZTO-LiF SSEs. (Dotted regions appeared darker pattern compared to LLZTO indicates that LiF is primarily located at grain boundaries)

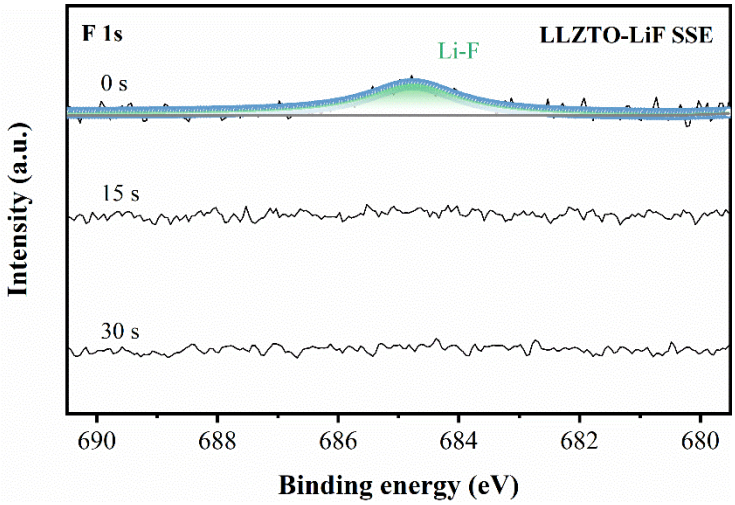

Fig. S3 XPS spectrums of LLZTO-LiF SSEs after Ar^+ etching 0s, 15s and 30s

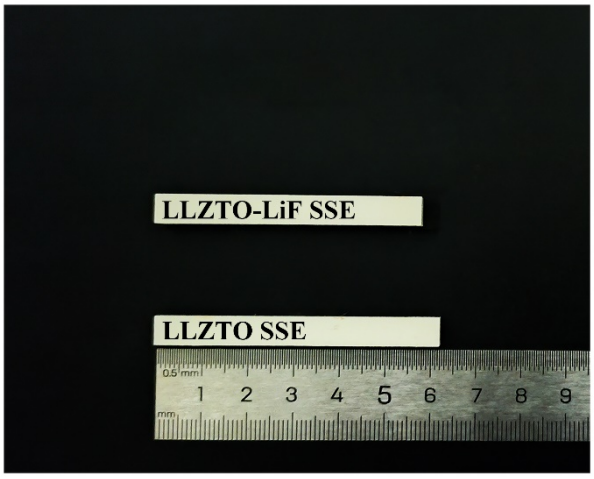

Fig. S4 Actual image of LLZTO and LLZTO-LiF ceramic strips after sintering.

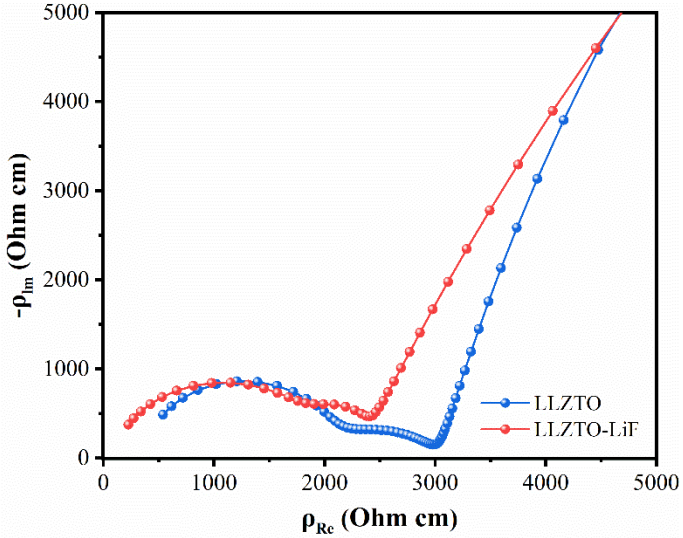

Fig. S5 EIS of different LLZTO SSEs at 5 °C.

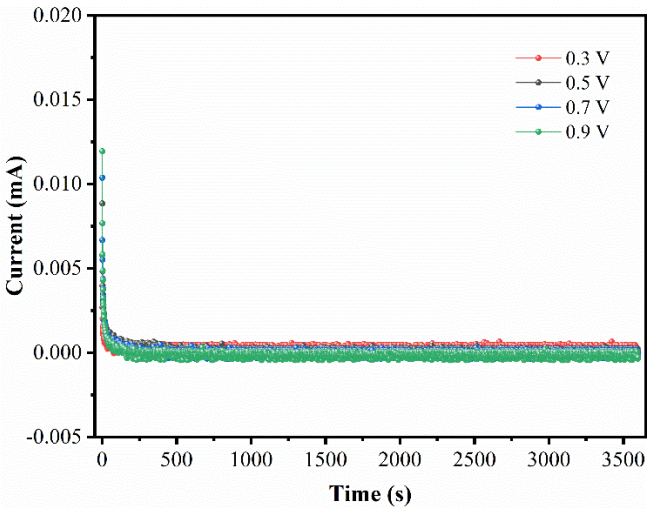

Fig. S6 DC polarization plots of LLZTO-LiF SSEs with different polarization voltage at 25 °C.

The Maxwell-Garnett model was applied to quantitatively analyze the bulk and grain boundary conductivities, correcting for the influence of density variations. The Maxwell-Garnett model describes the effective conductivity of a two-phase composite system, such as a dispersed medium within a host matrix. However, we believe that its conceptual framework can be reasonably extended to this study.

LLZTO is a typical lithium-ion conductor with high ionic conductivity, while LiF is an electronic insulator with extremely low electronic conductivity. At the microscopic level, LiF is primarily located at the grain boundaries, forming a system consisting of a lithium-ion-conductive matrix with insulating inclusions together with continuous LLZO grains, which aligns with the fundamental assumptions of the Maxwell-Garnett model for two-phase systems.[1] Furthermore, the introduction of LiF into the grain boundaries reduces porosity and improves the uniformity of the grain boundary structure, thereby enhancing the overall effective homogeneity of the system. On the macroscopic scale, the system can be approximated as an isotropic two-phase composite ionic conductor, which further supports the applicability of the Maxwell-Garnett model.[2] Finally, SEM (Fig. 3) and density measurements indicate that the volume fraction of LiF in the system is low. This sparse distribution of inclusions conforms to the basic assumption of the Maxwell-Garnett model regarding dispersed phases.[3]

The influence of LiF has been further considered in the following derivation. Regarding the determination of the volume fraction f used in the model, based on SEM and density measurements, the second phase in LLZTO SSEs is pores. Thus, the volume fraction is calculated as f_{LLZTO}=1−93.1%=0.069. In the case of LLZTO-LiF SSEs, the second phase is mainly LiF. Owing to the introduction of LiF, the relative density increases from 93.1% to 98.8%, leading to a volume fraction of $f_{LLZTO-LiF}$=98.8%−93.1%=0.057. The specific process is as follows:

$$\sigma_{eff} = \sigma_{bulk}\frac{\sigma_{second\ phase} + 2\sigma_{bulk} + 2f(\sigma_{second\ phase} - \sigma_{bulk})}{\sigma_{second\ phase} + 2\sigma_{bulk} - f(\sigma_{second\ phase} - \sigma_{bulk})}$$

where σ_{eff} represents the experimentally measured total conductivity, σ_{bulk} denotes the bulk conductivity after eliminating the influence of the second phase, and f is the

volume fraction of the second phase.

Given that the ionic conductivity of pores is nearly 0, the Maxwell-Garnett model of LLZTO SSEs can be simplified as follows:

$$\sigma_{eff,\ LLZTO} = \sigma_{bulk,\ LLZTO}\frac{1 - f_{LLZTO}}{1 + \frac{f_{LLZTO}}{2}}$$

Given that the ionic conductivity of LiF is less than 10^{-6} S cm^{-1},[4] which is considered non-negligible, the Maxwell-Garnett model applied to LLZTO-LiF SSEs is expressed as follows:

$$\sigma_{eff,LLZTO-LiF} = \sigma_{bulk,LLZTO-LiF}\frac{\sigma_{LiF} + 2\sigma_{bulk,LLZTO-LiF} + 2f_{LLZTO-LiF}(\sigma_{LiF} - \sigma_{bulk,\ LLZTO-LiF})}{\sigma_{LiF} + 2\sigma_{bulk,\ LLZTO-LiF} - f_{LLZTO-LiF}(\sigma_{LiF} - \sigma_{bulk,LLZTO-LiF})}$$

The total conductivity of SSEs is typically separated into bulk conductivity (σ_{bulk}) and grain boundary conductivity (σ_{gb}) using the Brick Layer Model.[5,6]

The σ_{bulk} and σ_{gb} of SSEs, corrected using the Maxwell-Garnett model, are presented in Table. 1.

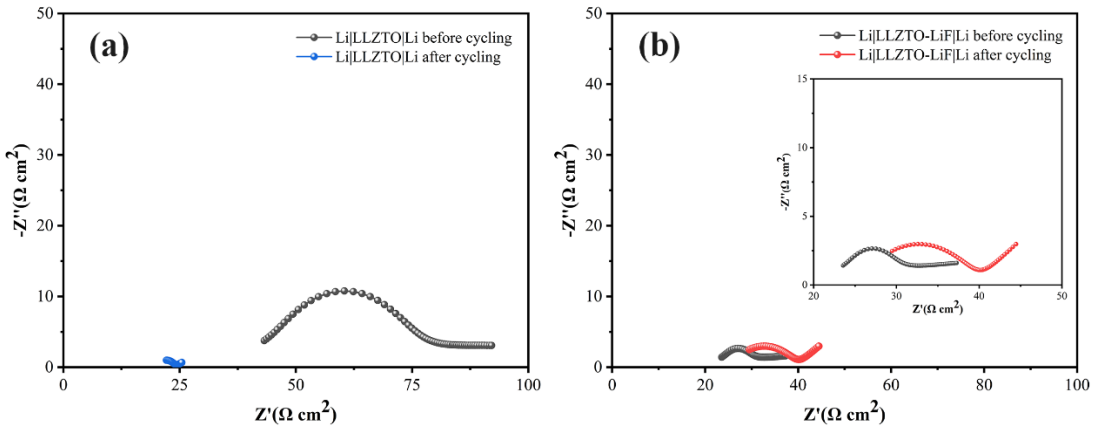

Fig. S7 EIS curves of (a) Li|LLZTO|Li and (b) Li|LLZTO-LiF|Li symmetric cells at before cycling and after cycling.

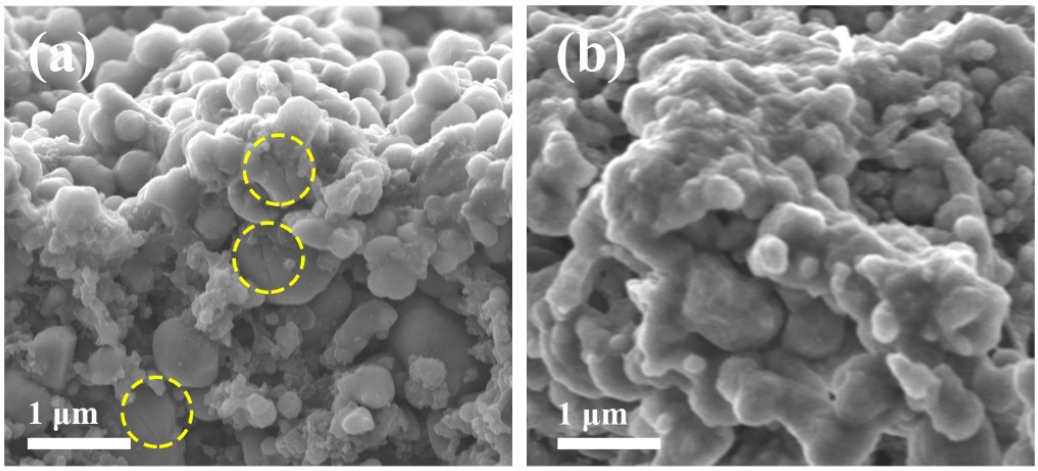

Fig. S8 SEM images of LFP cathode after cycling in SSLMBs.

(a) LFP cathode after cycling with LLZTO; (b) LFP cathode after cycling with LLZTO-LiF.

Table. S1 R_{bulk}, R_{gb}, σ_{bulk} and σ_{gb} for LLZO and LLZTO-LiF at 5 ℃.

Sample	LLZTO	LLZTO-LiF
R_{bulk} (Ω·cm)	2170	1904
R_{gb} (Ω·cm)	789	504
σ_{bulk} (S cm^{-1})	3.20×10^{-4}	4.02×10^{-4}
σ_{gb} (S cm^{-1})	8.81×10^{-4}	1.52×10^{-3}

Table. S2 Electronic conductivity of LLZTO-LiF SSEs with different polarization voltage.

Polarization voltage (V)	Electronic conductivity (S cm^{-1})
0.3	1.33×10^{-9}
0.5	1.21×10^{-9}
0.7	1.07×10^{-9}
0.9	0.98×10^{-9}

Table. S3 Cycle performance of Li|LLZTO-LiF|Li and its comparisons in previous reports of grain boundary modification.

Inorganic electrolyte	Modification phase	Current density (mA cm^{-2})	Cycling time (h)	Ref.
$Li_{6.5}La_3Zr_{1.5}Ta_{0.5}O_{12}$	Li_3PO_4	0.1	60	7
$Li_{6.75}La_3Zr_{1.75}Ta_{0.25}O_{12}$	LHE-LiCl	0.1	100	8
$Li_{6.4}La_3Zr_{1.4}Ta_{0.6}O_{12}$	Li_4SiO_4	0.1	260	9
$Li_{6.5}La_3Zr_{1.6}Ta_{0.4}O_{12}$	$LiAlO_2$	0.1	1000	10
$Li_7La_3Zr_2O_{12}$	LAF&$LiAlO_2$	0.1	4000	11
$Li_{6.5}La_3Zr_{1.5}Ta_{0.5}O_{12}$	$La_2Zr_2O_7$&MgO	0.2	350	12
$Li_{6.5}La_3Zr_{1.5}Ta_{0.5}O_{12}$	$LiGaO_2$	0.2	500	13
$Li_{6.5}La_3Zr_{1.45}Ta_{0.55}O_{12}$	Li_3N	0.2	500	14
$Li_{6.5}La_3Zr_{1.5}Ta_{0.5}O_{12}$	Li_2CuO_2	0.2	500	15
$Li_{6.4}La_3Zr_{1.4}Ta_{0.6}O_{12}$	PPA	0.2	1400	16
$Li_{6.4}La_3Zr_{1.4}Ta_{0.6}O_{12}$	LiF	0.1	8500	This work

References

1 J. P. Angle, Z. Wang, C. Dames and M. L. Mecartney, *J. Am. Ceram. Soc.*, 2013, **96**, 2935-2942.

2 Y. Cheng, X. Chen, K. Wu, S. Wu, Y. Chen and Y. Meng, *J. Appl. Phys.*, 2008, **103**, 034111.

3 A. Alexopoulos, *Phys. Lett. A*, 2009, **373**, 3190-3196.

4 S. Tang, G. Chen, F. Ren, H. Wang, W. Yang, C. Zheng, Z. Gong and Y. Yang, *J. Mater. Chem. A*, 2021, **9**, 3576-3583.

5 J. Fleig and J. Maier, *J. Electrochem. Soc.*, 1998, **145**, 2081.

6 J.-H. Hwang, D. S. McLachlan and T. O. Mason, *J. Electroceram.*, 1999, **3**, 7-16.

7 B. Xu, W. Li, H. Duan, H. Wang, Y. Guo, H. Li and H. Liu, *J. Power Sources*, 2017, **354**, 68-73.

8 Z. Zhang, L. Zhang, C. Yu, X. Yan, B. Xu and L.-m. Wang, *Electrochim. Acta*, 2018, **289**, 254-263.

9 S. Zhang, H. Zhao, J. Wang, T. Xu, K. Zhang and Z. Du, *Chem. Eng. J.*, 2020, **393**, 124797.

10 C.-C. Wang, W.-C. Hsu, C.-Y. Chang, M. Ihrig, N. T. Thuy Tran, S.-k. Lin, A. Windmüller, C.-L. Tsai, R.-A. Eichel and K.-F. Chiu, *J. Power Sources*, 2024, **602**, 234394.

11 J. Biao, B. Han, Y. Cao, Q. Li, G. Zhong, J. Ma, L. Chen, K. Yang, J. Mi, Y. Deng, M. Liu, W. Lv, F. Kang and Y. B. He, *Adv. Mater.*, 2023, **35**.

12 J. Lin, L. Wu, Z. Huang, X. Xu and J. Liu, *J. Energy Chem.*, 2020, **40**, 132-136.

13 W. Jeong, S. S. Park, J. Yun, H. R. Shin, J. Moon and J.-W. Lee, *Energy Storage Mater.*, 2023, **54**, 543-552.

14 M. Hong, Q. Dong, H. Xie, B. C. Clifford, J. Qian, X. Wang, J. Luo and L. Hu, *ACS Energy Lett.*, 2021, **6**, 3753-3760.

15 C. Zheng, J. Su, Z. Song, T. Xiu, J. Jin, M. E. Badding and Z. Wen, *J. Alloys Compd.*, 2023, **933**, 167810.

16 B.-Q. Xiong, Q. Nian, X. Zhao, Y. Chen, Y. Li, J. Jiang, S. Jiao, X. Zhan and X. Ren, *ACS Energy Lett.*, 2023, **8**, 537-544.